

Strong Continuation, Contrast Invariant Inpainting with a 3rd Order, *Optimal* PDE

Marcelo Bertalmío

Abstract

PDE-based image inpainting has become a very active area of research after the pioneering works of Masnou and Morel [1], Bertalmío et al. [2] and Ballester et al. [3]. In this paper we take a different approach, inspired by the excellent work of Caselles et al. [4]. We view the inpainting problem as a particular case of image interpolation in which we intend to propagate level lines. Expressing this in terms of local neighborhoods and using a Taylor expansion we derive a third order PDE that performs inpainting. This PDE is *optimal* in the sense that it is the most accurate third order PDE which can ensure continuation of level lines. The continuation is *strong*, allowing to restore thin structures occluded by a wide gap. The result is also contrast invariant. This is a novel PDE, which both in its accuracy and contrast invariance outperforms the approaches cited above.

Index Terms

Inpainting, Partial Differential Equations, Image Restoration.

I. INTRODUCTION

The modification of images in a way that is non-detectable for an observer who does not know the original image is called *retouching* or *inpainting*. Mainly three groups of works can be found in the literature related to digital inpainting. The first one deals with the restoration of films [5], the second one is related to texture synthesis [6], [7], [8], [9], and the third one is related to what we would call geometric inpainting. This article proposes a method to perform geometric inpainting, so let us comment on this latter category. For an extensive survey on geometric inpainting, see [10].

M. Bertalmío is with Departament de Tecnologia, Universitat Pompeu Fabra, Pg. de Circumvallació 8, 08003 Barcelona, Spain (e-mail: marcelo.bertalmio@upf.edu).

A pioneering contribution in the recovery of plane image geometry is due to D. Mumford, M. Nitzberg and T. Shiota [11], where the authors proposed an energy functional to segment a scene which took into account the depth of the objects in the scene and the energy of the occluded boundaries between T -junctions. They assumed that the completion curves should be as short as possible and should respect the *principle of good continuation* [12]: this principle is that contours based on smooth continuity are preferred to abrupt changes of direction. Inspired by the Elastica functional, Masnou and Morel [1], [13] proposed a variational formulation for the recovery of the missing parts of a gray level two-dimensional image and they referred to this interpolation process as *dis-occlusion*, since the missing parts can be considered as occlusions hiding the part of the image we want to recover. Their algorithm performs filling-in by joining with geodesic curves the points of the isophotes arriving at the boundary of the region to be in-painted.

Mumford's work on the Elastica Model and Masnou and Morel's contribution inspired Bertalmío, Sapiro, Caselles and Ballester [2] to propose an edge propagation PDE for the *Image Inpainting* formulation. Replicating basic art conservators techniques, a third order PDE propagates the level lines arriving at the missing region, and the completion tends to respect the *principle of good continuation*. Bertalmío, Bertozzi and Sapiro [14] showed the connection of this equation with Navier-Stokes equations, as well as a parallel among Image Processing and Fluid Dynamics quantities. On the other hand, Ballester, Bertalmío, Caselles, Sapiro and Verdera [3] introduced a relaxation of the Elastica functional which then can be minimized with a system of coupled PDE's: this is the first variational approach to the inpainting problem that complies with the *principle of good continuation* and is topologically independent.

A. Our contribution

The geometric inpainting methods just mentioned present some shortcomings that we intend to overcome. The *dis-occlusion* algorithm of Masnou [13] may connect boundary points with straight lines, thus not complying with the *principle of good continuation*. The *image inpainting* algorithm of Bertalmío et al. [2] is not contrast invariant, as it was pointed out by Chan et al. [15]. Chan et al. [15] propose a third order contrast invariant PDE for inpainting, with two competing terms in two orthogonal directions. The weights for these terms must be set manually, and they affect the *good continuation* of level lines. The *variational filling-in* of Ballester et al. [3] is not contrast invariant either, although contrast invariance is *imposed* in the implementation by decomposing each gray-level image into 256 binary images, one per level set, processing these binary images separately, and finally compositing these 256 results. Also from the standpoint of mathematical formality, these algorithms lack in some respects. *Dis-occlusion* and

variational filling-in come from approximations or relaxations of the Elastica functional, required since the functional is not lower semi-continuous, while the *image inpainting* equation intends to replicate the manual procedures of art conservators and its mathematical formality is an open question.

Our contribution in this article is the following. We reformulate the inpainting problem as a particular case of image interpolation in which we intend to propagate level lines. Expressing this in terms of local neighborhoods and using a Taylor expansion we derive a third order PDE that performs inpainting. This PDE is *optimal* in the sense that it is the most accurate third order PDE which can ensure *good continuation* of level lines. The continuation is *strong*, allowing to restore thin structures occluded by a wide gap. The result is also contrast invariant. This is a novel PDE, which both in its accuracy and contrast invariance outperforms the approaches cited above.

II. PROPOSED APPROACH

An image is usually modeled as a function I defined in a bounded domain $D \subseteq \mathbb{R}^2$ with values in \mathbb{R}^k ($k = 1$ for gray level images, or $k = 3$ for color images). For simplicity, we shall consider only the case of gray level images. The inpainting problem can be formulated generically in the following way. Given a subset Ω of the image domain D in which the values for I are not defined (the image *gap* that we wish to inpaint), we must determine values for I inside Ω which match the boundary conditions at $\partial\Omega$.

A. Inpainting as Interpolation

Inspired by the remarkable work by Caselles et al. [4] we will begin by reformulating the inpainting problem as a case of interpolation. Assume that the gap Ω contains only one pixel, x_0 . There are many possible criteria to choose the value $I(x_0)$ to fill the gap, let's recall from the introduction to [4] one of the simplest ones: *select $I(x_0)$ as the average of its level-line neighbors*. Then

$$I(x_0) = \frac{1}{2}(I(x_0 + hD^\perp I) + I(x_0 - hD^\perp I)), \quad (1)$$

with $D^\perp I$ the (counter-clockwise) 90 degree rotation of DI , the gradient of I (and therefore the level-line direction.) Expanding $I(x_0 + hD^\perp I)$ in a Taylor series:

$$\begin{aligned} I(x_0 + hD^\perp I) &= I(x_0) + \frac{h^2}{2}D^2I(D^\perp I, D^\perp I) + \\ &+ \frac{h^3}{6}D^3I(D^\perp I, D^\perp I, D^\perp I) + O(h^4), \end{aligned} \quad (2)$$

where we have omitted the pixel coordinate x_0 of I for simplicity, we have omitted the term for h because it is identically zero: $hD^\perp I \cdot DI \equiv 0$, and we have used the notation:

$$\begin{aligned} D^2 I(D^\perp I, D^\perp I) &= I_y^2 I_{xx} - 2I_x I_y I_{xy} + I_x^2 I_{yy}, \\ D^3 I(D^\perp I, D^\perp I, D^\perp I) &= I_y^2 (-I_y I_{xxx} + 3I_x I_{xxy}) + \\ &+ I_x^2 (-I_x I_{yyy} + 3I_y I_{yyx}). \end{aligned} \quad (3)$$

Averaging equation (2) with the similar equation we get when expanding $I(x_0 - hD^\perp I)$ we obtain:

$$\begin{aligned} \frac{1}{2}(I(x_0 + hD^\perp I) + I(x_0 - hD^\perp I)) &= I(x_0) + \\ \frac{h^2}{2} D^2 I(D^\perp I, D^\perp I) &+ O(h^4). \end{aligned} \quad (4)$$

Truncating this series and comparing with eq.(1), we obtain the following interpolation equation:

$$D^2 I(D^\perp I, D^\perp I) = 0. \quad (5)$$

A very important observation:

$$D^2 I(D^\perp I, D^\perp I) = \kappa(I) |DI|^3, \quad (6)$$

where $\kappa(I)$ is the Euclidean curvature of the level line of I at the pixel location x_0 . Therefore, this type of interpolation may be achieved as the steady state of the second order PDE

$$I_t = \kappa(I) |\nabla I|, \quad (7)$$

an equation which is closely related to Total Variation minimization [16] and Perona and Malik's anisotropic diffusion [17]. One may use this equation to perform inpainting [15], but since the steady state is $\kappa = 0$ all the interpolated level lines will have zero curvature and therefore they will be straight lines. This is an important limitation, stemming from the fact that eq.(7) is a second order PDE. It has been proven that in order to match not only gray value but also level line angle at the boundary $\partial\Omega$ we need a PDE of at least third order [14].

In order to find an interpolation procedure that yields a third order PDE, we propose the following criteria, extending the ideas presented above: *select $DI(x_0)$ as the average of its level-line neighbors*. That is, now we are interpolating the *gradient* along the level lines, instead of the gray level. Since interpolation of gray levels yielded a second order PDE, we expect that interpolation of the gradient yields a third order PDE. This criteria may be formulated as

$$DI(x_0) = \frac{1}{2}(DI(x_0 + hD^\perp I) + DI(x_0 - hD^\perp I)), \quad (8)$$

which implies

$$\begin{aligned} I_x(x_0) &= \frac{1}{2}[I_x(x_0 + hD^\perp I) + I_x(x_0 - hD^\perp I)], \\ I_y(x_0) &= \frac{1}{2}[I_y(x_0 + hD^\perp I) + I_y(x_0 - hD^\perp I)]. \end{aligned} \quad (9)$$

The expansion for $I_x(x_0 + hD^\perp I)$ is:

$$\begin{aligned} I_x(x_0 + hD^\perp I) &= I_x(x_0) + hD^\perp I \cdot DI_x + \\ &+ \frac{h^2}{2}(I_y^2 I_{xxx} - 2I_x I_y I_{xxy} + I_x^2 I_{yyx}) + O(h^3). \end{aligned} \quad (10)$$

Expanding I_y , letting $h \rightarrow 0$, truncating the series and averaging we obtain:

$$\begin{aligned} &-I_y[I_x(x_0 + hD^\perp I) + I_x(x_0 - hD^\perp I)] + \\ &+ I_x[I_y(x_0 + hD^\perp I) + I_y(x_0 - hD^\perp I)] = \\ &= h^2 D^3 I(D^\perp I, D^\perp I, D^\perp I). \end{aligned} \quad (11)$$

Substituting eq.(9) in (11) we get

$$D^3 I(D^\perp I, D^\perp I, D^\perp I) = 0. \quad (12)$$

Equation (12) is a novel PDE that we introduce in this paper to perform contrast invariant inpainting. It is also the third order PDE that best approximates the *principle of good continuation*. We will comment on these aspects next.

B. Properties of our proposed equation

We started our derivation by imposing continuity of the gradient, with eq.(8). Therefore the solution to equation (12) will have continuous DI , in particular across the gap boundary $\partial\Omega$ (continuity along each level line.) This implies that $D^\perp I$, the direction of the level line, will also be continuous, i.e., the interpolated level lines will bend smoothly and not have any *kinks*. In other words, our proposed equation satisfies the *principle of good continuation*, as intended. Let us now show why this equation is the third order PDE that best satisfies this principle.

Let us now pose the inpainting problem as a case of interpolation in which we want to propagate inside Ω the level lines arriving at $\partial\Omega$ but *keeping the direction of the lines*. We may require constancy of the level lines direction in the following way:

$$I(x_0 + hD^\perp I) - I(x_0 - hD^\perp I) = 0. \quad (13)$$

Letting $h \rightarrow 0$, expanding in a Taylor series and truncating after the fourth order term, we get the same third order equation as before:

$$D^3 I(D^\perp I, D^\perp I, D^\perp I) = 0. \quad (14)$$

The left hand side is the term of the expansion corresponding to h^3 , the first term that is not identically zero (since the term for h is identically zero, and the terms for even powers h^2 and h^4 cancel out when subtracting.) Any third order PDE other than eq.(14) will *not* cancel this first term of the expansion of eq.(13). Therefore any other third order PDE will approximate eq.(13) with a higher error than eq.(14). In this sense is that we say that our proposed PDE is *optimal*.

It may be a bit surprising to arrive at the same equation by a seemingly different path, but in fact eqs.(13) and (8) both imply the same: that the direction of each level line should be continuous along that level line (i.e., that as a curve the level line should have no singularities.)

Another very interesting property is the following:

$$D^3 I(D^\perp I, D^\perp I, D^\perp I) = D(\kappa|DI|^3) \cdot D^\perp I. \quad (15)$$

This implies that solving our equation (12) amounts to propagating the quantity $\kappa|DI|^3$ along the level lines of the image. So our equation is quite similar to the *image inpainting* equation $D(\Delta I) \cdot D^\perp I$, where the quantity propagated along the level lines was the Laplacian, ΔI , see [2].

In practice we solve eq.(12) by finding the steady state solution of

$$I_t = \frac{I_y^2(-I_y I_{xxx} + 3I_x I_{xxy}) + I_x^2(-I_x I_{yyy} + 3I_y I_{yyx})}{(I_x^2 + I_y^2)^{\frac{3}{2}}}. \quad (16)$$

Equation (16) is also contrast invariant: if for an initial image I we obtain a solution S , then for a contrast modified initial image $g(I)$ we obtain the solution $g(S)$, for $g : \mathbb{R} \rightarrow \mathbb{R}$ any non-decreasing function. This is an important property for any geometric inpainting algorithm, since it guarantees that the inpainting result depends only on the geometry of the initial image I and not on its particular contrast. We refer the reader to the appendix for this proof. Equation (16) is not invariant to inversion of contrast, though; for this we would need to add a new term, which is also discussed in the appendix.

C. Numerical Implementation

We have implemented eq. (16) using an explicit, forward time, finite differences scheme with the Monotonized Central Difference slope limiter of Van Leer [18]. Experimentally we found that the explicit, forward time, upwind finite differences scheme of Osher and Sethian [19] was too diffusive for this equation. We didn't achieve good results with the Mc Cormack scheme either [20].

For the sake of clarity, let's rewrite eq. (16) as

$$I_t = \frac{\beta}{(I_x^2 + I_y^2)^{\frac{3}{2}}}, \quad (17)$$

where

$$\beta = I_y^2(-I_y I_{xxx} + 3I_x I_{xxy}) + I_x^2(-I_x I_{yyy} + 3I_y I_{yyx}). \quad (18)$$

Now we multiply and divide the right-hand side by $|\nabla I|$:

$$I_t = \frac{\beta}{(I_x^2 + I_y^2)^{\frac{4}{2}}} (I_x^2 + I_y^2)^{\frac{1}{2}}. \quad (19)$$

We use central differences for the computation of all derivatives in β and the dividing term $(I_x^2 + I_y^2)^{\frac{4}{2}}$. But for the multiplying term $(I_x^2 + I_y^2)^{\frac{1}{2}}$, we use the aforementioned slope limiter:

$$\begin{aligned} I_x(i, j) &= \minmod(I_{x_C}(i, j), \minmod(2I_{x_B}(i, j), 2I_{x_F}(i, j))) \\ I_y(i, j) &= \minmod(I_{y_C}(i, j), \minmod(2I_{y_B}(i, j), 2I_{y_F}(i, j))), \end{aligned} \quad (20)$$

where the sub-subindexes C, B, and F denote central, backward and forward differences respectively and the *minmod* function satisfies:

$$\minmod(a, b) = \text{sign}(a) * \max(0, \min(|a|, b * \text{sign}(a))). \quad (21)$$

We apply a non-linear scaling of I_t to increase the speed of convergence:

$$I_t = \text{sign}(I_t) |I_t|^{\frac{1}{3}}.$$

Also, we add some anisotropic diffusion to prevent instabilities (which appear as wild oscillations):

$$I_t = I_t + \alpha \kappa(I) |\nabla I|,$$

where the weight α is 0.01. These are the same techniques used in [2]. Unfortunately, we don't know clearly how these numerical *tricks* modify the properties of our solutions. In particular, if $\alpha > 0$ we can no longer claim that our solution satisfies 14. We must choose the minimal *alpha* that guarantees stability so that the distortion introduced is also small, as it can be observed in the examples in the following section. In our experiments we have found that the adding of some diffusion is absolutely necessary, at least with the numerical schemes that we have implemented. We are carrying out further research in the numerical implementation for our equation.

All the images take values in the range 0 to 255. The time step is 0.1 and convergence is achieved in a few thousand iterations, depending on the size of Ω . To speed convergence it is convenient to initialize the process with a few steps of Gaussian filtering or, for bigger Ω , to use a multi-resolution approach.

D. Examples

Figure 1 shows the image I to inpaint (left), and the results obtained with Total Variation (TV) (middle left), *image inpainting* (middle right) and our equation (right.) Notice how with TV the solution is a straight line (zero curvature) so there is no continuation at the boundary. As we mentioned, this

is what to expect when we use 2nd order PDE's. With *image inpainting* there is good continuation but also bending of the line. With our equation, the edge is strongly propagated inward and we are able to reconstruct a corner inside Ω . To have an idea of the scale: the long side of the black trapezoid is 120 pixels long. Notice also that the result is not so good on the left hand side: this is due to the numerical scheme and our choice of orthogonal gradient (counter-clockwise), which in this figure makes information flow into the gap at the top right, and flow out at the bottom.

Figure 2 shows clearly the strength of the continuation achieved by our equation. With *image inpainting* (middle) structures that are thinner than the width of the gap will tend to not be connected, as it is the case here. The same situation arises with the variational approach in [3]. With our equation, the black bar is connected although its width is 30 pixels and the height of the occluding rectangle is 90 pixels.

In figure 3 the result is close to what one would expect, although the white squares end up not touching each other. We hope to overcome this limitation with a better numerical scheme. Both this figure and the previous one have been binarized (thresholded at the middle gray value.)

Figure 4 shows the result of using our equation for the restoration of the U component in a $U+V$ decomposition of the image [21]. For the V component we have used the texture synthesis algorithm of Efros and Leung [6]. In some parts the restoration is quite good, while in others there is noticeable blur stemming from the inpainting of U . Texture synthesis techniques like [7] do not cause blurring, but on the other hand they don't deal well with curved boundaries, as mentioned in [7]. Notice also that for our algorithm topology is not an issue (the gap Ω has a hole).

Fig. 5 shows the result for a color image, where we have applied our equation to each channel separately, using a $YCrCb$ color model ¹. Notice in the details (bottom row) how several thin structures are preserved, like the zippers in the orange uniform. Also the boundaries are sharp, and there are no spurious colors in the restoration.

III. CONCLUSION AND FUTURE WORK

We have introduced a third order PDE to perform geometric inpainting on images. This PDE is *optimal* in the sense that it is the most accurate third order PDE which can ensure continuation of level lines. It is also contrast invariant. With this equation the edges are propagated inside the gap with minimum bending, allowing for the connection of thin structures occluded by a wide gap, and also the formation

¹We could think of using techniques as those in [22], [23] to work on the three channels simultaneously, but with our current formulation no spurious colors appear on the inpainted solution so there doesn't seem to be a need for this.

of corners. This is a novel PDE, which both in its accuracy and contrast invariance outperforms previous related approaches in the area. We are currently studying the mathematical properties of this equation regarding existence and uniqueness of solutions and its numerical implementation.

APPENDIX

Be $g : \mathbb{R} \rightarrow \mathbb{R}$ a non-decreasing function. This is the contrast-modifying function that we apply to our image I . Therefore the partial derivatives take this form:

$$\begin{aligned}
g_t(I) &= g'(I)I_t \\
g_x(I) &= g'(I)I_x \\
g_{xx}(I) &= g''(I)I_x^2 + g'I_{xx} \\
g_{xy}(I) &= g''(I)I_xI_y + g'I_{xy} \\
g_{xxx}(I) &= g''(I)'(I)I_x^3 + 3g''(I)I_xI_{xx} + g'(I)I_{xxx} \\
g_{xxy}(I) &= g'''(I)I_yI_x^2 + g''(I)(2I_xI_{xy} + I_yI_{xx}) + g'(I)I_{xxy},
\end{aligned} \tag{22}$$

(for the remaining derivatives simply exchange the x and y subindexes.) Substituting I and its derivatives for g and its derivatives into eq. (16) and removing the terms that cancel out (those involving g'' and g''') yields:

$$\begin{aligned}
g'(I)I_t &= |g'(I)| \frac{I_y^2(-I_yI_{xxx} + 3I_xI_{xxy})}{(I_x^2 + I_y^2)^{\frac{3}{2}}} + \\
&+ |g'(I)| \frac{I_x^2(-I_xI_{yyy} + 3I_yI_{yyx})}{(I_x^2 + I_y^2)^{\frac{3}{2}}},
\end{aligned} \tag{23}$$

Since g is non-decreasing, $g' = |g'|$ and both eq. (23) and eq. (16) are the same. Therefore our proposed PDE eq. (16) is contrast invariant.

Notice that this is not the case if there is an inversion of contrast, so if $g' < 0$ then $(g(I))_t = -I_t$. To overcome this and make the equation also invariant to inversion of contrast, we have to multiply by a term that changes its sign when there is an inversion of contrast, and that does not alter the steady state of the equation. An example of such a term is the sign of the Euclidean curvature: $sg(\kappa)$, so our equation would be:

$$I_t = sg(\kappa)D(\kappa|DI|^3) \cdot D^\perp I, \tag{24}$$

which can be rewritten as

$$I_t = D(|\kappa||DI|^3) \cdot D^\perp I. \tag{25}$$

Unfortunately we have not obtained good experimental results with our numerical implementation of eq. (24), so all the experiments presented in this paper use eq. (16).

ACKNOWLEDGMENTS

This work is dedicated to Serrana Cabrera and Lucas Bertalmío. Many thanks to Vicent Caselles and Guillermo Sapiro for their help and suggestions. This work was partially supported by RACINE European Commission Project, Ramón y Cajal Program and PNP GC (BFM2003-02125).

REFERENCES

- [1] S. Masnou and J. Morel, “Level Lines Based Disocclusion,” in *Proc. 5th IEEE International Conference on Image Processing*, Chicago, Illinois, 1998, pp. 259–263.
- [2] M. Bertalmío, G. Sapiro, V. Caselles, and C. Ballester, “Image inpainting,” in *Proc. SIGGRAPH 00, ACM*, 2000, pp. 417–424.
- [3] C. Ballester, M. Bertalmío, V. Caselles, G. Sapiro, and J. Verdera, “Filling-in by Joint Interpolation of Vector Fields and Grey Levels,” *IEEE Transactions on Image Processing*, vol. 10, pp. 1200–1211, 2001.
- [4] V. Caselles, J. Morel, and C. Sbert, “An Axiomatic Approach to Image Interpolation,” *IEEE Transactions on Image Processing*, vol. 7, pp. 376–386, 1998.
- [5] A. Kokaram, “On missing data treatment for degraded video and film archives: a survey and a new bayesian approach,” *IEEE Transactions on Image Processing*, vol. 13, pp. 397–415, 2004.
- [6] A. Efros and T. Leung, “Texture synthesis by non-parametric sampling,” in *IEEE International Conference on Computer Vision*, 1999, pp. 1033–1038.
- [7] A. Criminisi, P. Perez, and K. Toyama, “Region filling and object removal by exemplar-based image inpainting,” *IEEE-TIP*, vol. 13, no. 9, pp. 1200–1212, 2004.
- [8] J. Jia and C. Kang, “Inference of segmented color and texture description by tensor voting,” *IEEE-TPAMI*, vol. 26, no. 6, pp. 771–786, 2004.
- [9] M. Elad, J. Starck, D. Donoho, and P. Querre, “Simultaneous cartoon and texture image inpainting using morphological component analysis (MCA),” *Applied and Computational Harmonic Analysis*, preprint, to appear 2005.
- [10] N. Paragios, Y. Chen, and O. Faugeras, Eds., *Mathematical models in computer vision: the handbook*. Springer, 2005, ch. PDE-based image and surface inpainting.
- [11] M. Nitzberg, D. Mumford, and T. Shiota, *Filtering, Segmentation, and Depth*. Springer-Verlag, Berlin, 1993.
- [12] G. Kanizsa, *Gramática de la Visión*. Paidós, 1986.
- [13] S. Masnou, “Disocclusion: a Variational Approach using Level Lines,” *IEEE Transactions on Image Processing*, vol. 11, pp. 68–76, 2002.
- [14] M. Bertalmío, A. Bertozzi, and G. Sapiro, “Navier-Stokes, fluid-dynamics, and image and video inpainting,” in *Proc. of IEEE-CVPR*, 2001, pp. 355–362.
- [15] T. Chan and J. Shen, “Morphologically invariant PDE Inpaintings,” University of California Los Angeles CAM Report, Tech. Rep., 2001.
- [16] L. Rudin, S. Osher, and E. Fatemi, “Nonlinear Total Variation Based Noise Removal Algorithms,” *Physica D*, vol. 60, pp. 259–268, 1992.
- [17] P. Perona and J. Malik, “Scale-space and edge detection using anisotropic diffusion,” *IEEE Transaction on Pattern Analysis and Machine Intelligence*, vol. 12, pp. 629–639, 1990.

- [18] B. Van Leer, "Towards the ultimate conservative difference scheme," *Journal of Computational Physics*, vol. 135, no. 2, pp. 229–248, 1997.
- [19] S. Osher and J. Sethian, "Fronts propagating with curvature dependent speed: algorithms based on Hamilton-Jacobi formulations," *Journal of Computational Physics*, vol. 79, pp. 12–49, 1988.
- [20] J. Hoffman, *Numerical methods for engineers and scientists*. Mc Graw Hill, 1992.
- [21] M. Bertalmío, L. Vese, G. Sapiro, and S. Osher, "Simultaneous structure and texture image inpainting," *IEEE-TIP*, vol. 12, no. 8, pp. 882–889, 2003.
- [22] B. Tang, G. Sapiro, and V. Caselles, "Diffusion of general data on non-flat manifolds via harmonic maps theory: The direction diffusion case," *International Journal of Computer Vision*, vol. 36, no. 2, pp. 149–161, 2000. [Online]. Available: citeseer.ist.psu.edu/tang00diffusion.html
- [23] D. Tschumperle and R. Deriche, "Regularization with PDE s : A common framework for different applications," *IEEE Transaction on Pattern Analysis and Machine Intelligence*, vol. 27, 2005.



Fig. 1. Image I to inpaint (left), results with TV (middle left), *image inpainting* equation (middle right), our equation (right).

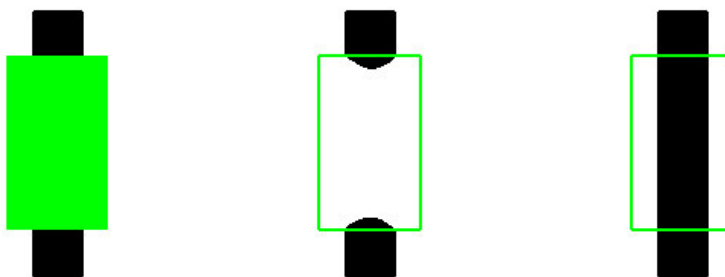


Fig. 2. Strong continuation property. Left: original; middle: result with *image inpainting* equation; right: result with our equation.



Fig. 3. Strong continuation property. Left: original; middle: thresholded result; right: result with our equation.

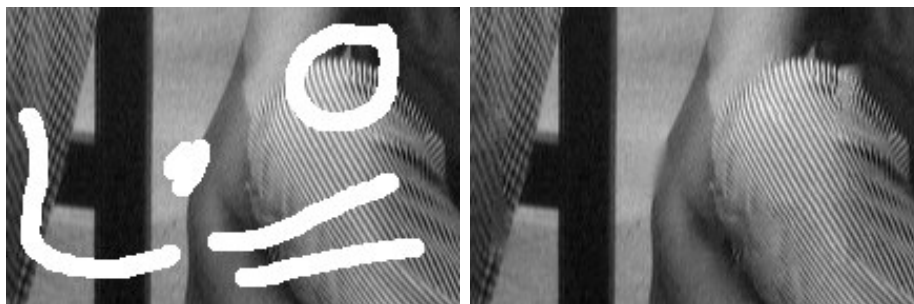


Fig. 4. Left: original (left). Right: results using our equation to restore the *structure* part of the image, see [21].



Fig. 5. Original (top left), restored (top right), detail (bottom row). Photo courtesy of Magela Ferrero.